

<https://helda.helsinki.fi>

Analysis of exocyst function in endodermis reveals its widespread contribution and specificity of action

Hematy, Kian

2022-06-01

Hematy , K , De Bellis , D , Wang , X , Mähönen , A P & Geldner , N 2022 , ' Analysis of exocyst function in endodermis reveals its widespread contribution and specificity of action ' , Plant Physiology , vol. 189 , no. 2 , pp. 557-566 . <https://doi.org/10.1093/plphys/kiac019>

<http://hdl.handle.net/10138/344546>

<https://doi.org/10.1093/plphys/kiac019>

cc_by_nc_nd

publishedVersion

Downloaded from Helda, University of Helsinki institutional repository.

This is an electronic reprint of the original article.

This reprint may differ from the original in pagination and typographic detail.

Please cite the original version.

Analysis of exocyst function in endodermis reveals its widespread contribution and specificity of action

Kian Hématy,^{1,2,†,*} Damien De Bellis ,^{1,3} Xin Wang ,^{4,5} Ari Pekka Mähönen ^{4,5} and Niko Geldner ^{1,†}

- 1 Department of Plant Molecular Biology, University of Lausanne, Lausanne 1015, Switzerland
- 2 Institut Jean-Pierre Bourgin, INRAE, AgroParisTech, Université Paris-Saclay, 78000 Versailles, France
- 3 Electron Microscopy Facility, University of Lausanne, Lausanne 1015, Switzerland
- 4 Institute of Biotechnology, HiLIFE, University of Helsinki, Helsinki 00014, Finland
- 5 Faculty of Biological and Environmental Sciences and Viikki Plant Science Centre, Organismal and Evolutionary Biology Research Programme, University of Helsinki, Helsinki 00014, Finland

*Author for correspondence: kian.hematy@inrae.fr

†Senior authors

K.H. designed the project, performed the experiments, analyzed the data, and wrote the manuscript. D.D.B. performed the TEM analysis. X.W. and A.P.M. provided the material and comments on the manuscript. N.G. participated in the experimental design and manuscript writing.

The author responsible for distribution of materials integral to the findings presented in this article in accordance with the policy described in the Instructions for Authors (<https://academic.oup.com/plphys/pages/General-Instructions>) is: Niko Geldner niko.geldner@unil.ch.

Abstract

The exocyst is the main plasma membrane vesicle-tethering complex in eukaryotes and is composed of eight different subunits. Yet, in plant genomes, many subunits display multiple copies, thought to reflect evolution of complex subtypes with divergent functions. In *Arabidopsis thaliana* root endodermal cells, the isoform EXO70A1 is required for positioning of CASP1 at the Casparian Strip Domain, but not for its non-targeted secretion to the plasma membrane. Here, we show that *exo84b* resembles *exo70a1* mutants regarding CASP1 mistargeting and secretion of apoplastic proteins, but *exo84b* additionally affects secretion of other integral plasma membrane proteins. Moreover, conditional, cell-type-specific gene editing of the single-copy core component SEC6 allows visualization of secretion defects in plant cells with a complete lack of exocyst complex function. Our approach opens avenues for deciphering the complexity/diversity of exocyst functions in plant cells and enables analysis of central trafficking components with lethal phenotypes.

Introduction

Membrane trafficking is essential for eukaryotic cells growth and cytokinesis. Transport of integral membrane proteins from the endoplasmic reticulum (ER) to plasmamembrane (PM) via the Golgi apparatus relies on vesicular trafficking and requires the function of numerous proteins along the way (Schekman and Novick, 2004; Schekman, 2010). This plethora of proteins support ER budding, vesicular transport to the target membranes where the vesicle will be tethered,

docked and fused, releasing the embedded membrane proteins and luminal content (Kanazawa and Ueda, 2017). Pioneering work from Novick and Schekman identified key factors involved in this process by forward genetics in the yeast *Saccharomyces cerevisiae* leading to the identification of 23 SEC loci (Novick and Schekman, 1979; Novick et al., 1980). Since then, the number of proteins involved in secretory processes has further expanded involving over 100 players (Schekman, 2010) and spatiotemporal regulation of secretion events is now accepted to be essential for correct

Received August 02, 2021. Accepted December 07, 2021. Advance access publication January 31, 2022

© The Author(s) 2022. Published by Oxford University Press on behalf of American Society of Plant Biologists.

This is an Open Access article distributed under the terms of the Creative Commons Attribution-NonCommercial-NoDerivs licence (<https://creativecommons.org/licenses/by-nc-nd/4.0/>), which permits non-commercial reproduction and distribution of the work, in any medium, provided the original work is not altered or transformed in any way, and that the work is properly cited. For commercial re-use, please contact journals.permissions@oup.com

Open Access

protein function, regulating their activation, stability and localization to various membrane locations. SEC3, SEC5, SEC6, SEC8, SEC10, SEC15, EXO70, and EXO84 proteins work together as subunits in a complex termed the exocyst. The exocyst is a vesicle-tethering complex conserved in eukaryotes and plays a key role in the last steps of secretion at the plasma membrane (Vukašinović and Žárský, 2016; Saeed et al., 2019). Whereas in the *S. cerevisiae* genome single genes encode each subunit, plant genomes have expanded their numbers, from a couple of isoforms for most subunits, up to several dozen for the EXO70 subunit (e.g. 23 isoforms in *Arabidopsis thaliana* and 41 in rice *Oryza sativa*). This large gene expansion of EXO70 suggests a functional diversification and specialization of the exocyst in plants, driven by the diversity of this subunit (Saeed et al., 2019; Žárský et al., 2020). Recent studies revealed indeed unique function for some EXO70 isoforms in targeting specific cargoes to discrete places in different plant cell types. Thus EXO70A1 is required for the localization of CASP1 proteins (Roppolo et al., 2011) at the Casparian Strip Domain (CSD) but not for its secretion to the plasma membrane per se (Kalmbach et al., 2017). In other words, EXO70A1 appears to be uniquely required for CASP1 targeted secretion to the CSD, but other EXO70 subunits can replace it for secretion to other domains of the plasma membrane. This idea is further supported by correct secretion of other protein cargoes such as SYP122 (SYNTAXIN122, [Pfister et al., 2014]), BOR1 (Takano et al., 2005), PDR6 (PLEIOTROPIC DRUG RESISTANCE 6, [Pfister et al., 2014]), PER64 (PEROXIDASE 64, [Lee et al., 2013]), or ESB1 (ENHANCED SUBERIN 1, [Hosmani et al., 2013]) in endodermal cells of *exo70a1* mutant (Kalmbach et al., 2017). Similarly EXO70H4 has a unique function in secreting autofluorescent compounds in leaf trichomes, as *exo70h4* mutant could only be complemented by expressing EXO70H4 but not by any 18 other EXO70 *Arabidopsis* isoforms tested (Kulich et al., 2018). Additionally, EXO70A1 and EXO70H4 are differentially localized in *Arabidopsis* trichomes: EXO70A1 labels the plasma membrane at the trichome base, whereas EXO70H4 is rather localized at its apex (Kubátová et al., 2019). Together these studies suggest the presence of different, functionally divergent, exocyst complex subtypes co-existing in plant cells.

Since the endodermis is an easily observed cell-type, with plasma membrane subdomains distinguished by clearly defined markers, we thought to define the function of distinct exocyst complexes by carrying out a reverse genetic approach. Our aim was to identify different exocyst subtypes required for secretion of different set of markers in the root endodermis. We investigated the contribution of different exocyst subunits involved in EXO70A1-dependent localization of CASP1 at the CSD or in EXO70A1-independent secretion of other protein cargoes. In this study, we identify the EXO84B isoform as an essential component for both the localization of CASP1 at the CSD and for the secretion of other tested integral membrane proteins to the PM, distinguishing it from EXO70A1. Interestingly, we found that

EXO84B is dispensable for the secretion of the apoplastic markers PER64 and ESB1. Therefore, these latter proteins are likely secreted by the two other EXO84 isoforms, EXO84A and EXO84C. Yet, both were still correctly secreted in an *exo84a/c* double mutant, suggesting that they can either use any of the three EXO84 subunits, or are secreted in an exocyst-independent fashion. The lethality of full knock-outs of exocyst function makes this question difficult to address and has been a major obstacle in understanding exocyst function in plants. We, therefore, decided to use a cell-type specific and inducible genome editing (IGE) system. With this, we demonstrate that all tested endodermal cargoes require a functional exocyst complex, since conditional gene editing of the unique exocyst subunit SEC6 affects their secretion in endodermal cells. Thus, our study reveals differential contribution of plant EXO84 isoforms for secretion and demonstrates the essential role the exocyst for general secretion in plants.

Results

EXO84B is required for CASP1 positioning but not for its secretion

The *exo70a1/lotr2* mutant has been recovered from a genetic screen for mislocalization of the CSD-resident CASP1 proteins. In *exo70a1/lotr2* mutants CASP1-GFP fails to accumulate as a continuous narrow band at the CSD and is instead scattered in patches all over the plasma membrane (Kalmbach et al., 2017). In contrast, other integral membrane proteins tested (polar or not) are properly secreted in *exo70a1* (Kalmbach et al., 2017). This highlighted the unique function of EXO70A1 in CSD targeting, but also the functional redundancy with other EXO70 isoforms for secretion of unaffected protein cargoes. To further characterize the composition of the CASP1-targeting exocyst complex, we investigated the contribution of EXO84 isoforms in CASP1 secretion (Figure 1A). EXO84 is the second most expanded subunit (three isoforms EXO84A-C) after the EXO70 subunit (23 isoforms). Consistent with its higher expression level (Figure 1B), EXO84B appears to have a predominant role among the isoforms, as witnessed by the strong growth defect of *exo84b* mutants, while *exo84a* or *exo84c* mutants, although deeply conserved in the plant lineage (Supplemental Figure S1, note that EXO84C gene diverges earlier in evolutionary history) were indistinguishable from wild-type plants (Figure 1D). Single mutants in either *exo84a* or *exo84c* possess a functional apoplastic barrier as shown by blockage of the apoplastic tracer, propidium iodide (PI, Figure 1C and Supplemental Figure S1A). The strong developmental phenotype of *exo84b* mutants (Figure 1D) prevented a meaningful readout for the PI-block assay, so we investigated directly the localization of CASP1-GFP in *exo84b* mutant. Interestingly, *exo84b* mutant phenocopies *exo70a1-1* in still allowing secretion of CASP1-GFP to the PM, but again in a non-localized fashion, leading to scattered ectopic patches at the PM instead of being focalized at the CSD, similar to what is observed in *exo70a1* mutants (Figure 1E). However,

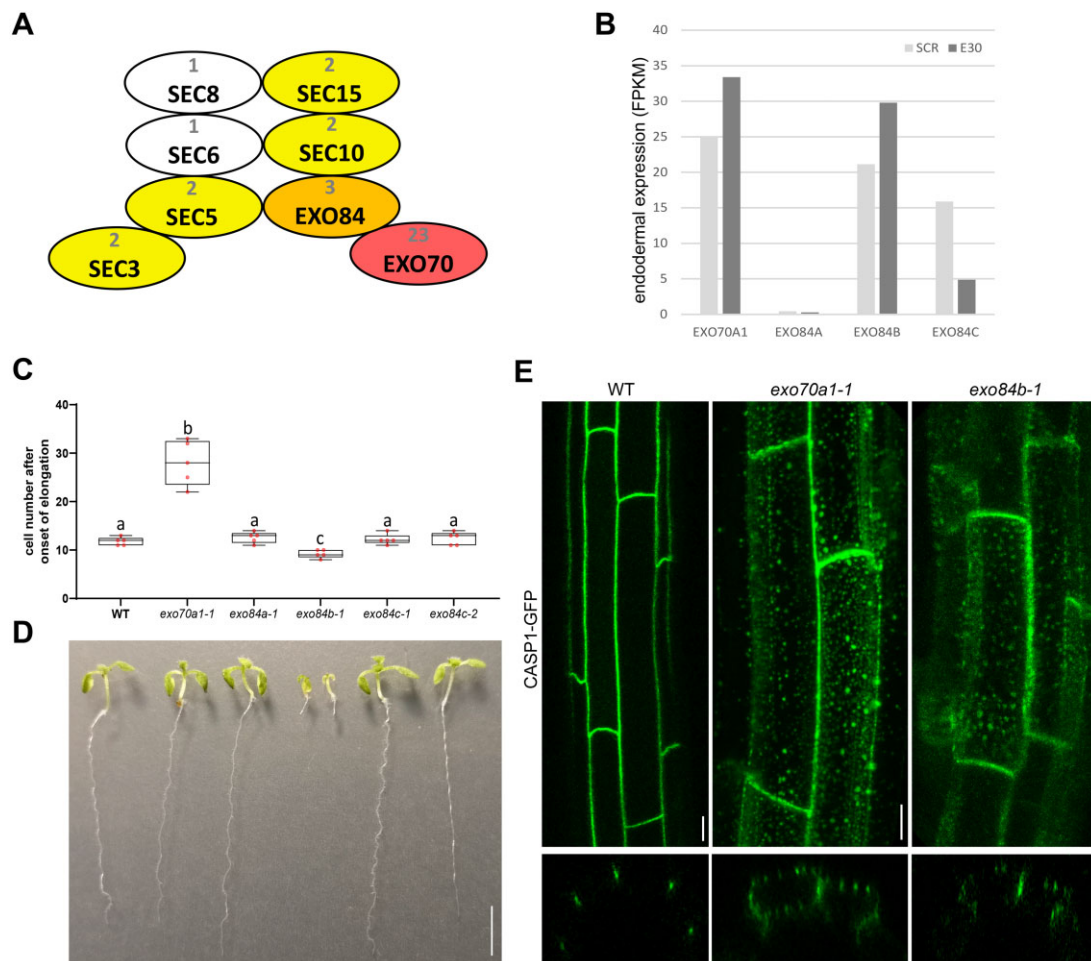


Figure 1 EXO84B is required, together with EXO70A1, for CASP1 positioning at the Casparian strip but not for its secretion at the plasma membrane. A, Schematic of the octameric exocyst holocomplex, gray numbers above subunit's name indicate number of isoforms in the Arabidopsis genome. Subunits are depicted in white when encoded by a unique gene and yellow, orange or red when encoded by 2, 3, or 23 isoforms, respectively. B, Expression in the endodermis of EXO84 isoforms compared to EXO70A1 from RNAseq analysis after cell sorting using pSCR or pE30 markers (adapted from Li et al., 2016, FPKM: Fragment per Kilobase per Million). C, Casparian Strip functionality assay using the apoplastic tracer PI. Different letters show statistical differences according to Tukey's HSD following one-way ANOVA ($P < 0.05$, $n = 5$). D, Picture of 7-d-old light-grown seedlings with their genotype indicated in the panel above. Bar = 5 mm. E, Localization of pCASP1: CASP1-GFP in root endodermal cells of 7-d-old seedlings of the indicated genotypes. Bar = 10 μ m.

CASP1 stability at the PM is greatly reduced in *exo84b* mutants and is only present in a few endodermal cells before its disappearance from the PM (Supplemental Figure S2A). This might be a secondary effect due to the strongly pleiotropic root growth defects of the mutant.

EXO84B function differentiates secretion of apoplastic and integral membrane proteins

Previous studies reported that *exo84b* mutants have a strong defect in secretion of plasma membrane marker Lti6b-GFP and polar membrane proteins PEN3 and NIP5;1, leading to their cytoplasmic accumulation in root epidermal cells (Mao et al., 2016). Puzzled by the PM-localization of CASP1 (albeit in a non-localized fashion) in *exo84b* endodermal cells, we investigated the secretion of a set of proteins targeted to various PM domains of

endodermal cells in *exo84b* mutant background. The apolar plasma membrane marker SYNTAXIN 122 (SYP122, Figure 2A) and both inner (BOR1, Figure 2B) and outer (PDR6, Figure 2C) polar markers showed secretion defects in *exo84b* endodermal cells leading to intracellular accumulation. In *exo84b* mutants, those markers failed to clearly label the PM. Instead, mCherry-SYP122 and BOR1-mCitrine present a strong intracellular signal in endodermal cells (Figure 2, A and B), while PDR6 shows a rather weak signal mostly in the vacuole (Figure 2C). However, like CASP1-GFP, the apoplastic markers PER64-mCherry (Figure 2D) and ESB1-mCherry (Supplemental Figure S2C) are correctly secreted to the cell wall in *exo84b*, but expectedly fail to localize to the central Casparian strip (CS) region, reminiscent of what has been observed in *exo70a1/lotr2* mutants (Kalmbach et al., 2017).

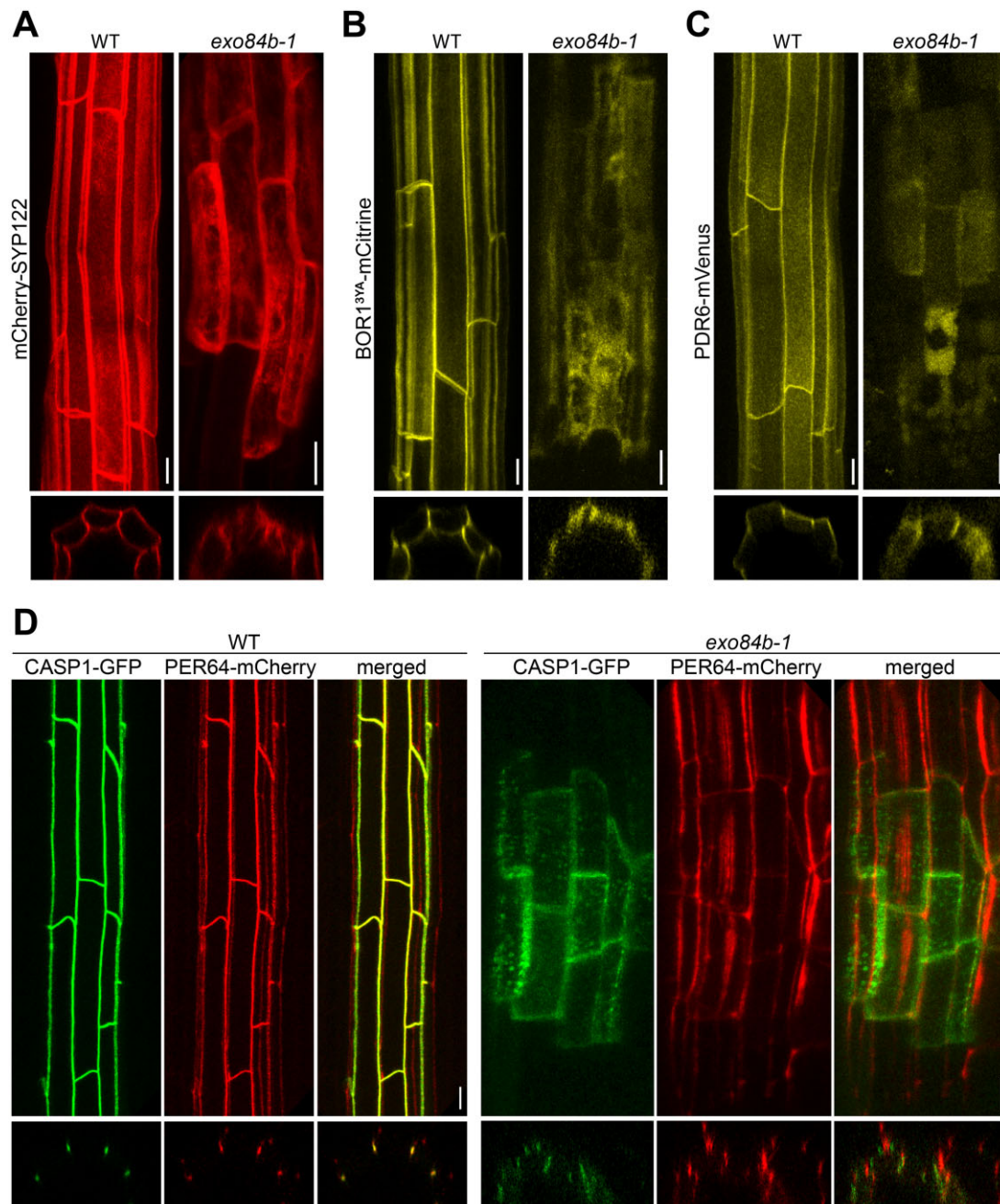


Figure 2 EXO84B is essential for secretion of integral membrane proteins, but is dispensable for secretion of apoplastic PER64 proteins. Effect of *exo84b* mutation on localization of apolar plasma membrane marker pCASP1:mCherry-SYP122 (A), inner polar marker pCASP1:BOR1^{3YA}-mCitrine (B), outer polar marker pCASP1:PDR6-mVenus (C) and apoplastic marker pCASP1:PER64-mCherry (D). Root endodermal cells from 7-d-old seedling. Upper panel corresponds to a maximum Z-projections covering half of the endodermis layer, lower panel corresponds to a transverse/orthogonal view from this image stack. Bar = 10 μ m.

EXO84A&C are dispensable for secretion of all tested markers

The observed secretion of CASP1 to ectopic patches at the PM and of PER64 to the apoplast in *exo84b* mutants could be attributed to the remaining expression of functional isoforms EXO84A&C. To investigate a possibly dedicated role of those isoforms in CASP1 and PER64 secretion, we expressed them in *exo84a exo84c* double mutant. Because of the close linkage of EXO84A and EXO84C on chromosome 1,

we generated a double mutant by CRISPR-Cas9 editing of EXO84C in an *exo84a-1* T-DNA insertion mutant (Supplemental Figure S3). Surprisingly, double mutants *exo84a-1 exo84c^{cr1}* display no obvious growth phenotype and both CASP1-GFP and PER64-mCherry are correctly secreted to the CSD and to the CS, respectively, in this background (Figure 3A). Thus, secretion of CASP1 and PER64 could be redundantly mediated by any of the EXO84 isoforms. Alternatively, their secretion might occur through an

entirely exocyst-independent pathway. Interestingly, despite these differences in secretion, both CASP1 and PER64 are sensitive to BFA-treatment (Figure 3B), as are PM-marker SYP122 and apoplastic ESB1 (Supplemental Figure S4, A and B). Thus secreted proteins, showing different requirement for exocyst function, are equally dependent on the ARF-GEF GNOM for their endosomal sorting.

Inducible endodermal editing of SEC6 demonstrates exocyst-dependent secretion of CASP1 and apoplastic proteins

To our knowledge, no secretion defect (i.e. intracellular accumulation) has yet been observed for CASP1 or any apoplastic proteins in viable exocyst mutants investigated (Kalmbach et al., 2017; Figures 2D and 3A). This leaves the protracted question whether, in those mutants, secretion occurs in an exocyst-independent manner, or whether a level of exocyst function necessary for viability is simply always sufficient to maintain secretion of CASP1 and apoplastic proteins. Indeed, stable genetic manipulation of non-redundant, core exocyst component is lethal, often at the male gametophytic stage, precluding straightforward cell biological analysis of strong exocyst knock-outs (Hála et al., 2008). Taking advantage of a recently developed IGE in plants (Wang et al., 2020), we generated IGE lines expressing, inducibly upon Estradiol application, the CRISPR-Cas9 protein in early differentiating endodermis to generate targeted mutations in the unique SEC6 gene in the Arabidopsis genome. Using the SCARECROW promoter to drive the expression of estrogen inducible XVE system (Siligato et al., 2016) would allow expression of Cas9 protein in meristematic endodermis upon Estradiol treatment (Wang et al., 2020). This should allow early editing of SEC6 locus in order to obtain homozygous *sec6* mutant before the onset of expression of the fluorescent markers that are under the expression of CASP1 promoter (active during early endodermal differentiation, Figure 4A). As expected from their dependency on EXO84B function (Figure 2), SYP122, BOR1, and PDR6 showed clear defects in secretion to the plasma membrane upon induction of SEC6 editing (Figure 4, B–D). Importantly, although not complete, we could observe a secretion defect for the apoplastic markers PER64 (Figure 4E) and ESB1 (Figure 4F) upon SEC6 mutation. Also for CASP1-GFP proteins, a weak intracellular accumulation is observed (Figure 4B; Hosmani et al., 2013; Kalmbach et al., 2017). However, we could not observe a complete disappearance of CASP1 from the CSD, nor of the apoplastic proteins from the cell wall, suggesting that editing either occurred either too late in endodermal development or that SEC6 proteins are particularly stable and remain present long after mutation of the SEC6 locus (Christiano et al., 2014). Nevertheless, we were able to obtain stable transgenic lines, showing a reproducible phenotype in the endodermis upon induction (Figure 4, B–F and Supplemental Figure S5). We could confirm editing at the SEC6 locus by extracting DNA from roots of transgenic lines after Cas9 induction and

performing Sanger sequencing of PCR amplicons spanning the region matching the targeting sgRNA^{SEC6} (Supplemental Figure S5, A and C–E).

Ultrastructural analysis reveals strong, cell-specific secretion defects in *sec6*-edited lines

Genetic interference with SEC6 by the IGE system leads to increased intracellular signal of the studied cargoes that either appear smooth/“cytosolic” (Figure 4B and Supplemental Figure S4B) or in the form of intracellular aggregates/patches (Figure 4, C–F). To gain further insight into the defects induced in those lines, we observed intracellular structures by electron microscopy of ultra-thin transverse sections of roots, performed after induction of SEC6 editing. We observed strong vesicle crowding in the cytoplasm of endodermal cells in two independent lines expressing the SEC6 IGE construct (Figure 5A), strikingly resembling the original, strong yeast exocyst mutants (Novick and Schekman, 1979). Importantly, neighboring pericycle cells appeared completely normal, impressively illustrating the cell-specificity of the inducible CRISPR/Cas9 system. This was confirmed by quantification of vesicles in the cytoplasm of endodermal and adjacent pericycle cells showing a 4–5 times increase in vesicle density specifically in the endodermis of IGE lines compared to induced-control cells (Figure 5B). No difference in vesicle density is observed in neighboring pericycle cells confirming the tissue-specificity of the IGE system in the endodermis. Additionally, using the IGE system targeting EXO84 genes, we could recapitulate the phenotypes observed in *exo84b* T-DNA allele (Supplemental Figure S6B), which differed from the secretion defect observed upon editing of SEC6. Furthermore, the lack of secretion defect upon editing of EXO84A or EXO84C genes excludes a possible effect of Cas9 itself in the phenotypes observed.

Discussion

The identification of EXO70A1 as an essential exocyst component for CASP1 positioning, but not for its secretion, suggested the existence of functionally divergent exocyst complex subtypes co-existing in the endodermis. This was further supported by the correct secretion and localization of other protein cargoes (namely SYP122, BOR1, PDR6, and PER64) tested in *exo70a1* mutants (Kalmbach et al., 2017). Here, we show that *exo84b* mutant is mimicking *exo70a1* mutant's phenotype regarding CASP1 positioning (Figure 1E). This demonstrates that EXO84B is required, together with EXO70A1, to target CASP1 to the CSD, which fits with the reported interaction between those two subunits (Fendrych et al., 2010). Yet, it also suggests that in *exo84b* mutants, the functional EXO70A1 protein is not able to associate with the other EXO84 isoforms expressed to achieve the localized secretion of CASP1. Thus, EXO70A1 is likely exclusively interacting with EXO84B to perform its function of targeting CASP1 to the CSD. Mutation of EXO84B also affects a broader set of protein cargoes

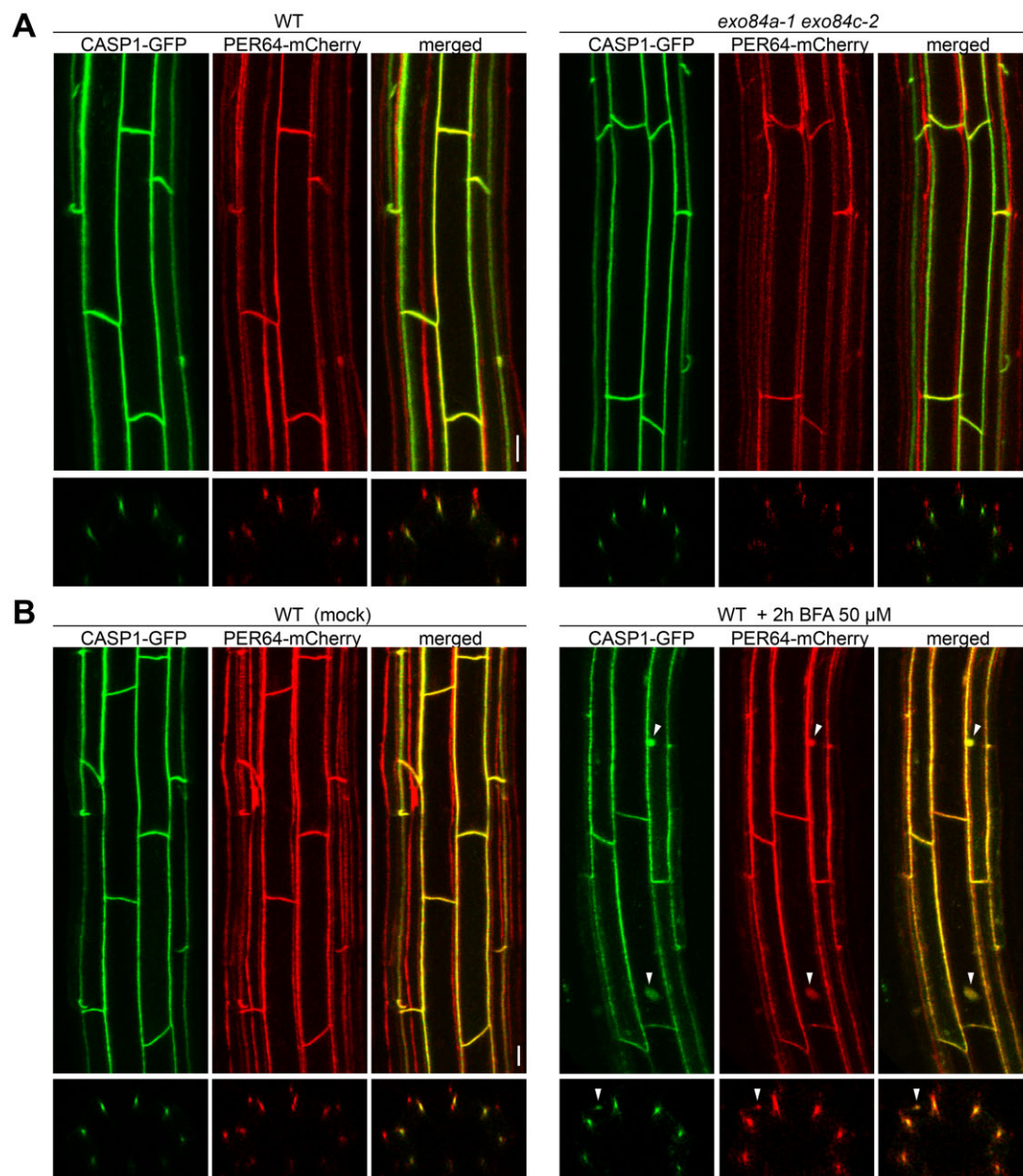


Figure 3 EXO84A&C isoforms are also dispensable for secretion of integral membrane protein CASP1 and apoplastic protein PER64. A, Both CASP1-GFP and PER64-mCherry are correctly secreted and localized in *exo84a/c* double mutants. B, Both CASP1 and PER64 are BFA-sensitive at the onset of their expression in the endodermis. Root endodermal cells from 7-d-old seedlings treated with 50 μM BFA for 2 h in 0.5 \times MS liquid medium. Upper panel corresponds to a maximum Z-projections covering half of the endodermis layer, lower panel corresponds to transverse/orthogonal view from this image stack. White arrowheads point to BFA-bodies. Bar = 10 μm .

(Figure 2, A–C) than seen in *exo70a1* mutants (Kalmbach et al., 2017), showing that EXO84B must be engaged in different exocyst complex subtypes (likely containing different EXO70 isoforms) and has a more essential/widespread function than EXO70A1 in plants cells. Consistently, *exo84b* mutants, display a much stronger growth defect than *exo70a1* mutants (Figure 1D).

Surprisingly, secretion of apoplastic proteins PER64 and ESB1 is not affected neither in *exo70a1* (Kalmbach et al., 2017) nor in *exo84b* mutants (Figure 2D and Supplemental Figure S2). This could be explained by functional

redundancy among the remaining EXO70 or EXO84 isoforms expressed in the endodermis of those mutants. Alternatively, secretion of apoplastic proteins could occur in an exocyst-independent manner unlike the PM proteins that strictly rely on it. The large number of EXO70 isoforms expressed in the endodermis (Kalmbach et al., 2017) complicates the genetic investigation of their putative redundancy. Hence, we investigated the role of EXO84A&C isoforms for apoplastic secretion. Like in *exo84b* mutants, PER64-mCherry remains properly secreted in *exo84a/c* double mutants (Figure 3), showing that EXO84A&C isoforms are not

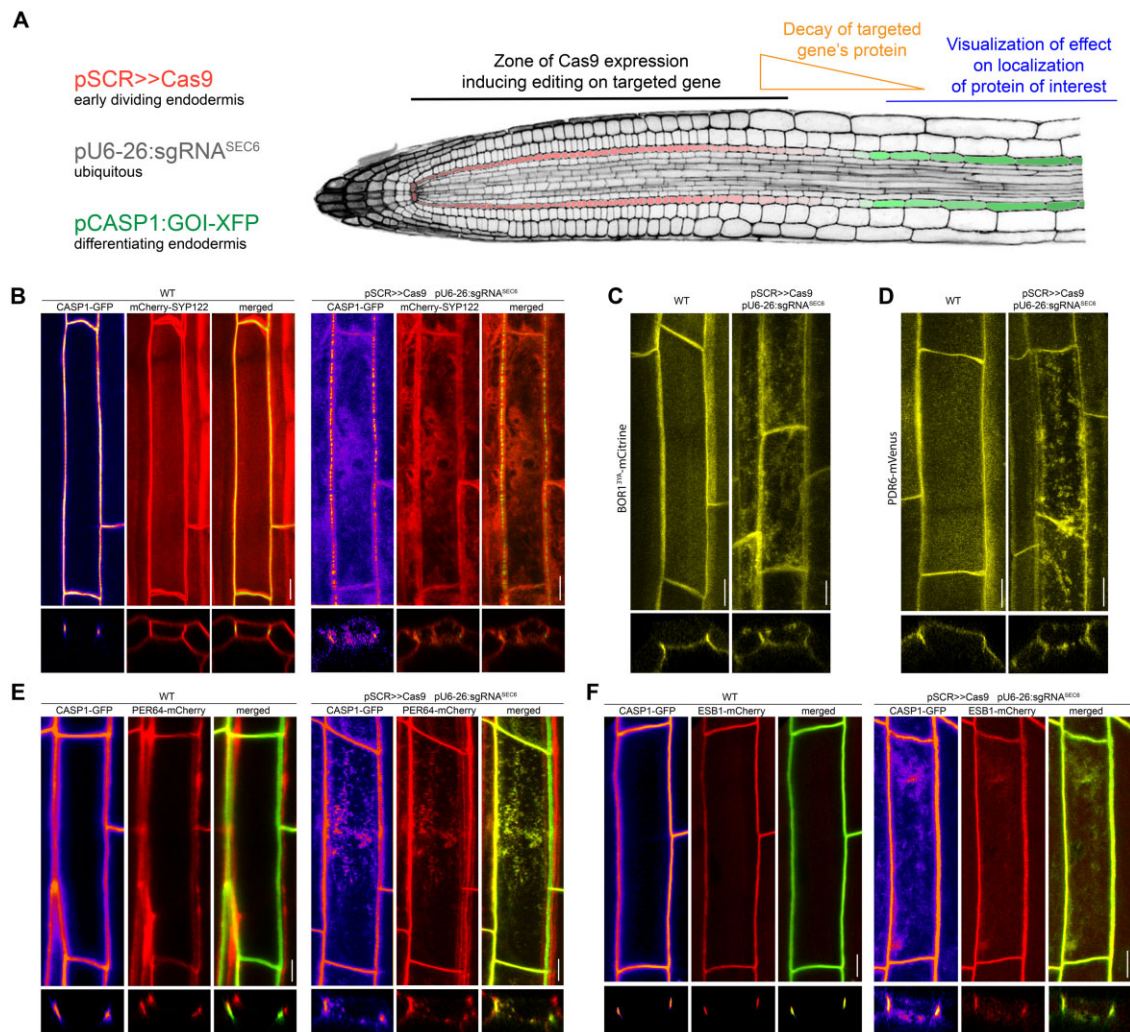


Figure 4 Use of tissue-specific inducible CRISPR allows assessment of exocyst-dependent secretion. A, Representation of a root tip expressing the IGE system for endodermal inducible editing of SEC6 and visualization of its effect in differentiated endodermis. Upon estradiol treatment, the pSCR:XVE will induce Cas9 expression (in red) in early endodermis, triggering *sec6* mutations independently in different endodermal cells. Once mutated clearing of existing endogenous SEC6 would occur to later reveal a phenotype on pCASP1-driven fluorescent marker lines. B–F, Effect of inducible endodermal Cas9-editing of exocyst subunit SEC6 on localization of apolar plasma membrane marker pCASP1:mCherry-SYP122 (B), inner polar marker pCASP1:BOR1^{3YΔ}-mCitrine (C), outer polar marker pCASP1:PDR6-mVenus (D) and apoplastic markers pCASP1:PER64-mCherry (E) and pESB1:ESB1-mCherry (F). Root endodermal cells from 7-d-old seedling were imaged by confocal microscopy after 2d induction on media containing 2 μM estradiol. Upper panel maximum Z-projections, lower panel orthogonal view. Bar = 10 μm.

dedicated to secretion of this apoplastic marker. However, whether PER64 secretion requires the redundant function of EXO84 isoforms or whether it occurs through an exocyst-independent mechanism still remained unclear. Due to its essential and widespread function, a complete lack of an exocyst subunit (i.e. “exocyst-deficient” mutant) is male gametophytic lethal, preventing analysis of homozygous mutant phenotype (Hála et al., 2008) and, very probably, the generation of an *exo84a/b/c* triple mutant.

Fortunately, the recent development of IGE tools (Wang et al., 2020) allowed us to generate endodermal cells completely lacking functional exocyst-complexes by targeting its uniquely encoded subunit SEC6. Using this system, we could thus demonstrate that, in *sec6* mutated cells, all investigated protein cargoes tested (including the apoplastic

ones) were dependent on exocyst function for their secretion (Figure 4). Consistently, we could observe by electron microscopy, the accumulation of vesicles in the cytoplasm of *sec6*-mutated endodermal cells (Figure 5), reminiscent of defect observed in *sec* mutants of *S. cerevisiae* (Novick and Schekman, 1979).

This work further illustrates the diversity of exocyst subunit function in plant cells. Particularly, it clarifies the requirement of EXO84 isoforms for secretion of many integral membrane proteins, but more specifically for CASP1 positioning at the CSD. Additionally, it reveals a differential requirement for EXO84 isoforms for secretion of some apoplastic proteins (e.g. PER64 and ESB1, Figures 2 and 3 and Supplemental Figures S2 and S6). Finally, our work reveals the power of IGE systems for addressing previously

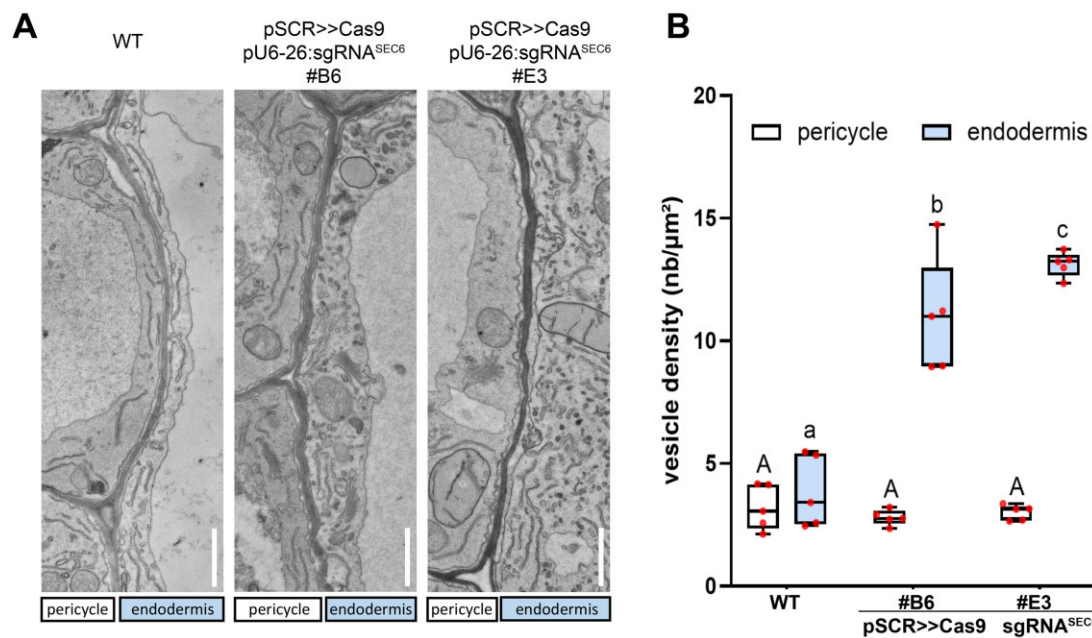


Figure 5 Ultrastructural analysis of SEC6-edited lines reveals vesicle crowding in the cytoplasm of endodermal cells. A, TEM micrographs of roots cells from the indicated genotypes showing the interface between pericycle and endodermal cells. Seedlings were all treated 2 d with 2 μ M estradiol prior to fixation for TEM analysis. Bar = 1 μ m. B, Quantification of vesicles in pericycle and endodermal cells of WT (Col pCASP1:CASP1-GFP; pCASP1:mCherry-SYP122) and two independent homozygous lines expressing pSCR>>Cas9 and pU6-26:sgRNA^{SEC6}. Both WT and inducible lines were treated for 2 d with 2 μ M estradiol prior to fixation for TEM analysis. 5–10 μ m² cytoplasmic areas from $n = 5$ cells of each cell types were analyzed from two roots of each genotype. Different letters (uppercase letters refer to pericycle, lowercase letters refer to endodermis) show statistical differences according to Tukey's HSD following one-way ANOVA ($P < 0.05$).

unanswerable questions, allowing to study essential gene functions in specific cell types in an otherwise normal organ and tissue context. This methodology is evidently widely applicable, but will be particularly useful for the study of intracellular trafficking, a field that has been repeatedly hampered by the inability to study strong vesicle trafficking in a cell-type of interest and in a normal developmental context, because of early lethality of mutants in many important trafficking regulators. This has too often forced research into the analysis of weak mutants, whose phenotypes can be often difficult to interpret.

Materials and methods

Plant material and growth conditions

Arabidopsis (*Arabidopsis thaliana*) ecotype Columbia was used for all experiments. For in vitro assays, seeds were stratified 2 d at 4°C in the dark, then germinated vertically for 7 d at 22°C under continuous light (100 μ E) on agar plates containing half-strength Murashige and Skoog (MS) medium. For induction of IGE lines, seedlings were grown for 5 d on 0.5 \times MS solid media and transferred for 2 d on 0.5 \times MS solid media supplemented with 2 μ M Estradiol. BFA treatments were performed on 7 d old seedling grown on 0.5 \times MS solid media transferred for 2 h in liquid 0.5 \times MS medium + 50 μ M BFA (or + 0.1% v/v DMSO as mock treatment).

The following mutants were used in this study: *exo70a1-1* (SALK_014826); *exo84a-1* (SALK_072277); *exo84b-1* (GABI_459C01); *exo84c-1* (SALK_011569).

The following transgenic lines pCASP1:CASP1-GFP/pCASP1:mCherry-SYP122 (Kalmbach et al., 2017); pCASP1:CASP1-GFP/pCASP1:PER64-mCh (Lee et al., 2013); pCASP1:CASP1-GFP/pESB1:ESB1-mCherry (Hosmani et al., 2013); pCASP1:BOR1^{3YA}-mCitrine (Kalmbach et al., 2017); and pCASP1:PDR6-mVenus (Kalmbach et al., 2017) were crossed with *exo84b-1* mutant or transformed with the IGE system constructs targeting SEC6. *exo84a-1exo84c-2* was generated by CRISPR editing of EXO84C in *exo84a-1* expressing pCASP1:PER64-mCh and further transformed with pCASP1:CASP1-GFP with FastRed selection cassette (Rojas-Murcia et al., 2020). Between two and four transgenic lines carrying a single T-DNA of each constructs (based on a 3/1 segregation ratio of the selection marker) were isolated for further characterization. A representative image is shown for confocal microscopy figures.

Gene Numbers: EXO70A1 (At5g03540); EXO84A (At1g10385); EXO84B (At5g49830); EXO84C (At1g10180); SEC6 (At1g71820).

Construct cloning

All constructs were generated using the Multisite Gateway Technology (Life Technologies, Carlsbad, CA, USA) and plant transformation performed according to the floral dip protocol (Clough and Bent, 1998) using *Agrobacterium*

tumefaciens GV3101 (pMP90). Generation of stably edited lines in EXO84C in *exo84a-1* has been done as described previously (Rojas-Murcia et al., 2020) with sgRNA^{EXO84C} described in Supplemental Figure S3 using primers listed in Supplemental Table S1. IGE constructs were assembled by LR reaction between a pDEST FR34GW (FastRed selection marker) and the pENTR vectors pL4L1r-pSCR:XVE/pLexA (Siligato et al., 2016), pL1L2-SpCas9:T35s (Wang et al., 2020), and pL2rL3-pU6-26-sgRNA with sgRNA^{SEC6} annealed primers (Supplemental Table S1) cloned at BbsI site by ligation (Rojas-Murcia et al., 2020).

Sequencing of CRISPR-edited lines

Stable mutants were generated as described (Rojas-Murcia et al., 2020), T1 lines were selected based on editing detected on DNA extracted from a rosette leaf after PCR amplicon Sanger sequencing. Homozygous mutants were selected from FastRed negative T2 plants showing monoallelic homozygous mutation.

For verification of SEC6 editing in IGE lines, seedlings were induced as described above. Genomic DNA was extracted from the lower half of 7d old roots (~1 cm long segment) and SEC6 amplicon were sent for Sanger sequencing (cf. Supplemental Figure S5) allowing to detect frameshift symptomatic of base pair deletion due to Cas9-editing at the predicted position of the sgRNA targeting SEC6 locus.

Fluorescence microscopy

Confocal laser-scanning microscopy experiments were performed either on a Leica SP8 equipped with an Argon Laser and a white light laser. GFP/mCherry were acquired in sequential mode with 488/561 nm excitation and detection parameters 490–530/590–630 nm, respectively. mCitrine or mVenus fluorophores were acquired with 514 nm excitation and a 520–560 nm detection window.

For the apoplastic barrier functionality assay, 7-d-old seedlings were incubated 5 min with PI (10 mg/mL). Quantification was performed by confocal microscopy, visualizing PI with 561 nm excitation and 600–650 nm detection. The “onset of endodermal elongation” was defined as the point where the length of an endodermal cell in a median optical section was more than three times its width. From this point, cells in the file were counted until the endodermal cells blocked the PI penetration to the stele.

Electron microscopy

Plants were fixed in glutaraldehyde solution (EMS, Hatfield, PA, USA) 2.5% in phosphate buffer (PB 0.1 M [pH 7.4]) for 1 h at RT and postfixed in a fresh mixture of osmium tetroxide 1% (EMS) with 1.5% of potassium ferrocyanide (Sigma, St. Louis, MO, USA) in PB buffer for 1 h at RT. The samples were then washed twice in distilled water and dehydrated in ethanol solution (Sigma) at graded concentrations (30%—40 min; 50%—40 min; 70%—40 min; 100%—2 × 1 h). This was followed by infiltration in Spurr resin (EMS) at graded concentrations (Spurr 33% in ethanol—4 h; Spurr 66% in ethanol—4 h; Spurr 100%—2 × 8 h) and finally polymerized

for 48 h at 60°C in an oven. For the multiple mutant, ultrathin sections of 50 nm thick were cut transversally at 2 mm above the root tip, using a Leica Ultracut (Leica Mikrosysteme GmbH, Vienna, Austria), picked up on a copper slot grid 2 × 1 mm (EMS) coated with a polystyrene film (Sigma). Micrographs and panoramic were taken with a transmission electron microscope FEI CM100 (FEI, Eindhoven, The Netherlands) at an acceleration voltage of 80 kV with a TVIPS TemCamF416 digital camera (TVIPS GmbH, Gauting, Germany) using the software EM-MENU 4.0 (TVIPS GmbH). Panoramic were aligned with the software IMOD (Kremer et al., 1996).

Statistical analysis

Statistical significance was assessed using one-way ANOVA, followed by post hoc analysis with Tukey's HSD test at $\alpha < 0.05$. All statistical analyses were performed in Graphpad PRISM version 8. In the box plots, the boxes indicate the first and third quartiles, the lines represent the median values, the whiskers indicate minimal and maximal values, and the points represent individual measurements.

Accession numbers

Sequence data from this article can be found in the GenBank/EMBL data libraries under the accession numbers listed in Supplemental Table S1.

Supplemental data

The following materials are available in the online version of this article.

Supplemental Figure S1. Gene structure, T-DNA mutants used, and phylogeny of Arabidopsis EXO84 isoforms.

Supplemental Figure S2. Arabidopsis *exo84b-1* mutants expressing CASP1-GFP and ESB1-mCherry.

Supplemental Figure S3. *exo84a/c* mutant generation.

Supplemental Figure S4. SYP122 and ESB1 are BFA-sensitive.

Supplemental Figure S5. Characterization of SYP122 *sec6* IGE lines.

Supplemental Figure S6. Characterization of *exo84* IGE lines.

Supplemental Table S1. Primers used in this study.

Acknowledgments

We would like to thank members of the Geldner laboratory for stimulating discussion during the course of this project.

Funding

K.H. has received the support of the EU in the framework of the Marie-Curie FP7 COFUND People Program, through the award of an AgreeSkills+ fellowship (under grant agreement no. FP7-609398). This work was supported by two consecutive SNSF grants (project numbers 176399 and 156261) to N.G.

Conflict of interest statement. None declared.

References

- Brinkman EK, Chen T, Amendola M, Van Steensel B** (2014) Easy quantitative assessment of genome editing by sequence trace decomposition. *Nucleic Acids Res* **42**: e168 doi: 10.1093/nar/gku936
- Christiano R, Nagaraj N, Fröhlich F, Walther TC** (2014) Global proteome turnover analyses of the yeasts *S. cerevisiae* and *S. pombe*. *Cell Rep* **9**: 1959–1965
- Clough SJ, Bent AF** (1998) Floral dip: a simplified method for *Agrobacterium*-mediated transformation of *Arabidopsis thaliana*. *Plant J* **16**: 735–43
- Fendrych M, Žárský V, Synek L, Pečenková T, Toupalová H, Cole R, Drdová E, Nebesářová J, Sedínová M, Hála M, et al.** (2010) The *Arabidopsis* exocyst complex is involved in cytokinesis and cell plate maturation. *Plant Cell* **22**: 3053–3065
- Hála M, Cole R, Synek L, Drdová E, Pečenková T, Nordheim A, Lamkemeyer T, Madlung J, Hochholdinger F, Fowler JE, et al.** (2008) An exocyst complex functions in plant cell growth in *Arabidopsis* and tobacco. *Plant Cell* **20**: 1330–1345
- Hosmani PS, Kamiya T, Danku J, Naseer S, Geldner N, Guerinot M, Lou Salt DE** (2013) Dirigent domain-containing protein is part of the machinery required for formation of the lignin-based Casparian strip in the root. *Proc Natl Acad Sci USA* **110**: 14498–14503
- Kalmbach L, Hématy K, De Bellis D, Barberon M, Fujita S, Ursache R, Daraspe J, Geldner N** (2017) Transient cell-specific EXO70A1 activity in the CASP domain and Casparian strip localization. *Nat Plants* **3**: 17058 doi: 10.1038/nplants.2017.58
- Kanazawa T, Ueda T** (2017) Exocytic trafficking pathways in plants: why and how they are redirected. *New Phytol* **215**: 952–957
- Kremer JR, Mastrorarde DN, McIntosh JR** (1996) Computer visualization of three-dimensional image data using IMOD. *J Struct Biol* **116**: 71–76
- Kubátová Z, Pejchar P, Potocký M, Sekereš J, Žárský V, Kulich I** (2019) *Arabidopsis* trichome contains two plasma membrane domains with different lipid compositions which attract distinct EXO70 subunits. *Int J Mol Sci* **20**: 3803 doi: 10.3390/ijms20153803
- Kulich I, Vojtková Z, Sabol P, Ortmannová J, Neděla V, Tihlaříková E, Žárský V** (2018) Exocyst subunit EXO70H4 has a specific role in callose synthase secretion and silica accumulation. *Plant Physiol* **176**: 2040–2051
- Kumar S, Stecher G, Li M, Knyaz C, Tamura K** (2018) MEGA X: molecular evolutionary genetics analysis across computing platforms. *Mol Biol Evol* **35**: 1547–1549
- Lee Y, Rubio MC, Allassimone J, Geldner N** (2013) A mechanism for localized lignin deposition in the endodermis. *Cell* **153**: 402–412
- Mao H, Nakamura M, Viotti C, Grebe M** (2016) A framework for lateral membrane trafficking and polar tethering of the PEN3 ATP-binding cassette transporter. *Plant Physiol* **172**: 2245–2260
- Novick P, Field C, Schekman R** (1980) Identification of 23 complementation groups required for post-translational events in the yeast secretory pathway. *Cell* **21**: 205–215
- Novick P, Schekman R** (1979) Secretion and cell-surface growth are blocked in a temperature-sensitive mutant of *Saccharomyces cerevisiae*. *Proc Natl Acad Sci USA* **76**: 1858–1862
- Pfister A, Barberon M, Allassimone J, Kalmbach L, Lee Y, Vermeer JEM, Yamazaki M, Li G, Maurel C, Takano J, et al.** (2014) A receptor-like kinase mutant with absent endodermal diffusion barrier displays selective nutrient homeostasis defects. *Elife* **3**: e03115
- Rojas-Murcia N, Hématy K, Lee Y, Emonet A, Ursache R, Fujita S, de Bellis D, Geldner N** (2020) High-order mutants reveal an essential requirement for peroxidases but not laccases in Casparian strip lignification. *Proc Natl Acad Sci USA* **117**: 29166–29177
- Roppolo D, De Rybel B, Tendon VD, Pfister A, Allassimone J, Vermeer JEM, Yamazaki M, Stierhof YD, Beeckman T, Geldner N** (2011) A novel protein family mediates Casparian strip formation in the endodermis. *Nature* **473**: 381–384
- Saeed B, Brillada C, Trujillo M** (2019) Dissecting the plant exocyst. *Curr Opin Plant Biol* **52**: 69–76
- Schekman R** (2010) Charting the secretory pathway in a simple eukaryote. *Mol Biol Cell* **21**: 3781–3784
- Schekman R, Novick P** (2004) 23 genes, 23 years later. *Cell* **116**: S13–S15 doi: 10.1016/s0092-8674(03)00972-3
- Siligato R, Wang X, Yadav SR, Lehesranta S, Ma G, Ursache R, Sevilem I, Zhang J, Gorte M, Prasad K, et al.** (2016) Multisite gateway-compatible cell type-specific gene-inducible system for plants. *Plant Physiol* **170**: 627–641
- Takano J, Miwa K, Yuan L, von Wirén N, Fujiwara T** (2005) Endocytosis and degradation of BOR1, a boron transporter of *Arabidopsis thaliana*, regulated by boron availability. *Proc Natl Acad Sci USA* **102**: 12276–12281
- Vukasinić N, Žárský V** (2016) Tethering complexes in the *Arabidopsis* endomembrane system. *Front Cell Dev Biol* **4**: 46
- Wang X, Ye L, Lyu M, Ursache R, Löytynoja A, Mähönen AP** (2020) An inducible genome editing system for plants. *Nat Plants* **6**: 766–772
- Žárský V, Sekereš J, Kubátová Z, Pečenková T, Cvrčková F** (2020) Three subfamilies of exocyst EXO70 family subunits in land plants: early divergence and ongoing functional specialization. *J Exp Bot* **71**: 49–62